Supplementary Information

Ratiometric Red-emission Fluorescent Detection of Al^{3+} in Pure Aqueous Solution and Live Cells by Fluorescent Peptidyl Probe using Aggregation-Induced emission

Lok Nath Neupane [a], Pramod Kumar Mehta[a], Semin Oh[a], See-Hyoung Park[b], Keun -Hyeung Lee[a,*]

[a]Center for Design and Applications of Molecular Catalysts, Department of Chemistry and Chemical Engineering, Inha University, Incheon, 402-751, South Korea.
[b]Department of Bio and Chemical Engineering, Hongik University, Sejong 30016, South Korea.

Email address: leekh@inha.ac.kr
Fax number: +82-32-8675604
Phone number: +82-32-8607674

Contents:

DLS measurement and CD measurement

The size distribution in an aqueous buffered solution (1 mM Tris, pH 7.0) was measured using a laser diffraction particle size analyzer (ELSZ, Otsuka Electronics, Osaka, Japan). The measurements were carried out by 90° dynamic light scattering at 25 ℃.

Circular dichroism experiments were performed using JASCO 815 CD spectropolarimeter (Jasco, Tokyo, Japan). All the data were collected from 600 to 350 nm at a scan rate of 100 nm/min at 0.5 nm data intervals and are presented as an average of three successive scans unless specified.

Determination of detection limit and dissociation constant

The detection limit of **1** to Al^{3+} was calculated based on a fluorescence titration. To determine the S/N ratio, the fluorescence emission intensity ratio (I_{600}/I_{535}) of 5 μM of **1** in aqueous solutions was measured 10 times, and the standard deviation of the blank measurements was determined. Three separate measurements of the emission intensity ratio were measured in the presence of increasing Al^{3+} concentrations, and the mean intensity ratio was plotted as a function of the Al^{3+} concentration to determine the slope. The detection limit was calculated using the following equation:

$$\text{Detection limit} = 3\sigma/m$$

where σ is the standard deviation of the intensity ratio of **1** in the absence of Al^{3+}, and m is the slope of the emission intensity ratio (I_{600}/I_{535}) of 5 μM of **1** as a function of the Al^{3+} concentration.[1]

The dissociation constant was calculated based on the titration curve of the probe with metal ion. The fluorescence signal, F, is related to the equilibrium concentration of the complex (HL) between Host (H) and metal ion (L) by the following expression:

$$F = F_o + \Delta F \times [HL]$$

$$[HL] = 0.5\times [K_D + L_T + H_T - \{(- K_D - L_T - H_T)^2 - 4 L_T H_T\}^{1/2}]$$

where F_o is the fluorescence of the probe only and ΔF is the change in fluorescence due to the formation of HL. The dissociation constant was determined by a nonlinear least square fit of the data with the equation.[2] The dissociation constant was calculated based on fluorescence titration curve of the probe with the metal ion using the modified Benesi-Hildebrand equation. The dissociation constant was calculated using the following equation.[3,4]

$$\text{Log}(I_x - I_0/I_{max} - I_0) = n\times\log[M] - \log K_d$$

where I_0 is the fluorescence of the probe only, I is the change in fluorescence due to the formation of complex, I_{max} is the final fluorescence emission intensity, M is the concentration of Al^{3+} ions, and n is the slope.

Measurement of Quantum yields

Fluorescence quantum yields of **1** in the presence and absence of Al^{3+} were obtained by using fluorescein as a standard. Each of the sample solution were prepared in distilled water and the absorbance were recorded in 10 mM tris buffer solution in different 10 mm quartz cell. The fluorescence spectrums of the solutions were recorded with the excitation wavelength of 470 nm and the relative fluorescence was determined by the area of the fluorescence emission. Where fluorescein used as a standard and its known quantum yield value is 0.91.[5] Finally, quantum yield of **1** in the absence and presence of Al^{3+} were calculated.[6]

Transmission Electron Microscopy (TEM) measurements

Transmission electron microscopy (TEM) was performed using a Philips CM 200 operated at an acceleration voltage of 120 kV. The sample was prepared by dropping 5 μL of the complex of **1** and Al^{3+} on a 300-mesh copper grid coated with carbon followed by staining with phosphotungstic acid (1 wt%). TEM grids were completely dried in vacuum desiccator before TEM measurements.

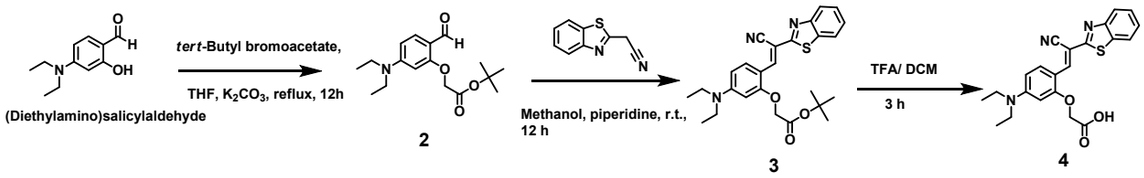

Scheme S1. Synthetic scheme of **4**

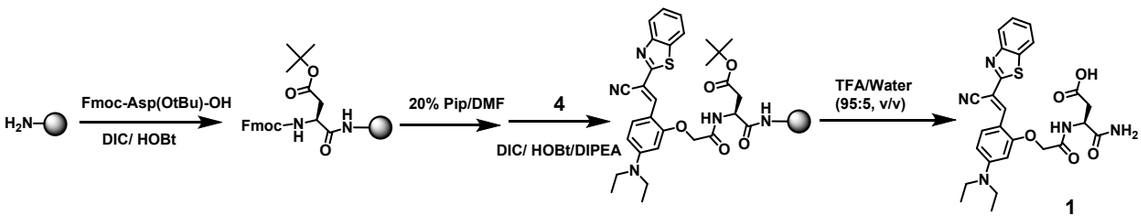

Scheme S2. Synthetic scheme of **1**

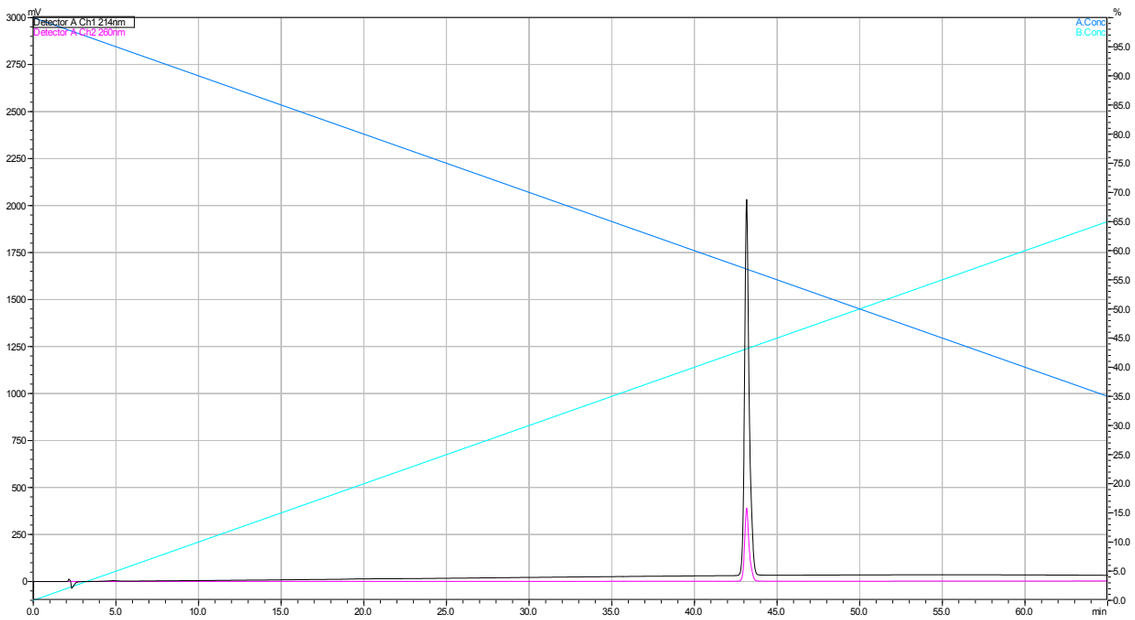

Fig. S1. HPLC chromatogram of **4**

+MS, 0.1-0.4min #3-22

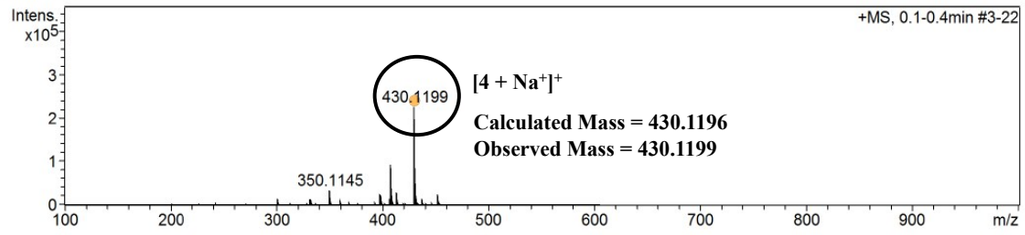

Meas. m/z	#	Ion Formula	m/z	err [ppm]	mSigma	# Sigma	Score	rdb	e¯ Conf	N-Rule
430.1199	1	C20H16N9OS	430.1193	-1.5	5.7	1	100.00	17.5	even	ok
	2	C19H20N5O5S	430.1180	4.6	7.8	2	41.47	12.5	even	ok
	3	C24H20N3O3S	430.1220	4.7	18.1	3	32.44	16.5	even	ok
	4	C18H24NO9S	430.1166	-7.7	19.2	4	10.00	7.5	even	ok
	5	C17H20N9OS2	430.1227	-6.3	21.2	5	21.32	12.5	even	ok
	6	C16H24N5O5S2	430.1213	-3.2	27.3	6	52.40	7.5	even	ok
	7	C19H28NO4S3	430.1175	5.7	44.3	7	15.26	6.5	even	ok
	8	C16H32NO4S4	430.1209	-2.1	64.0	8	23.81	1.5	even	ok
	1	C18H17N9NaOS	430.1169	-7.1	5.8	1	15.30	14.5	even	ok
	2	C22H21N3NaO3S	430.1196	0.8	7.4	2	100.00	13.5	even	ok
	3	C19H25N3NaO3S2	430.1230	7.0	23.0	3	14.19	8.5	even	ok
	4	C27H21NNaOS	430.1236	-8.5	30.0	4	4.89	17.5	even	ok

Fig. S2. HRMS (ESI-TOF) spectrum of **4**

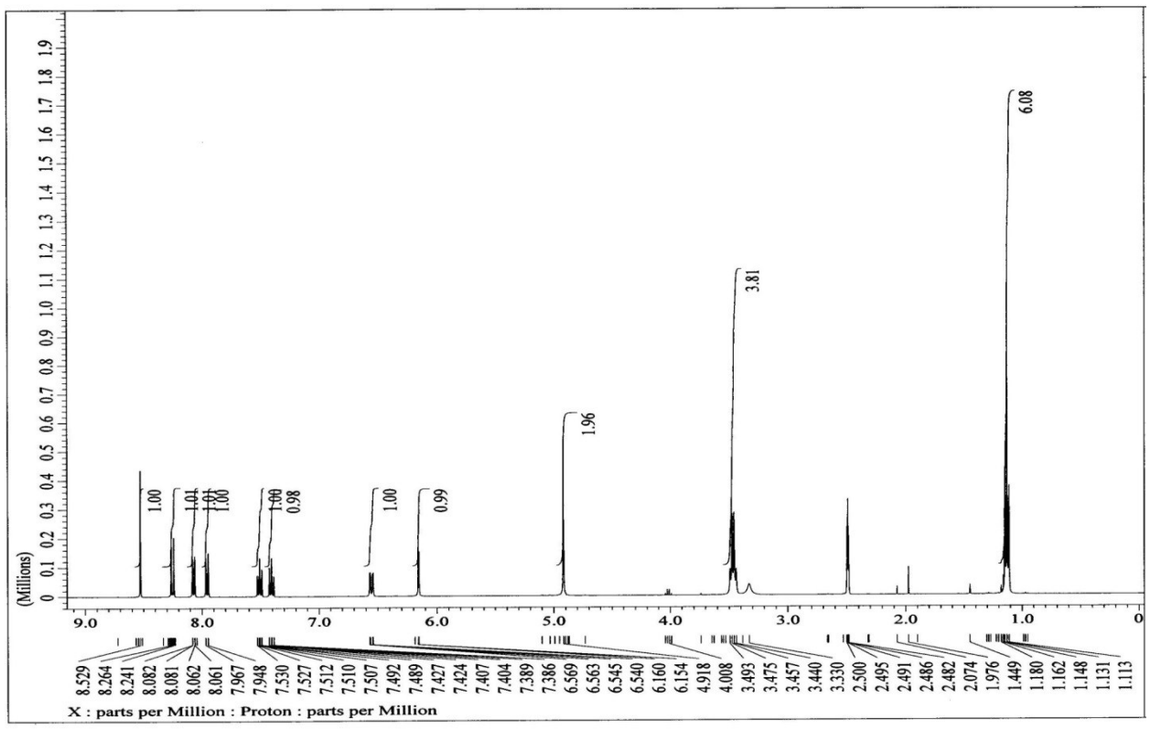

Fig. S3. ^{1}H NMR of **4**

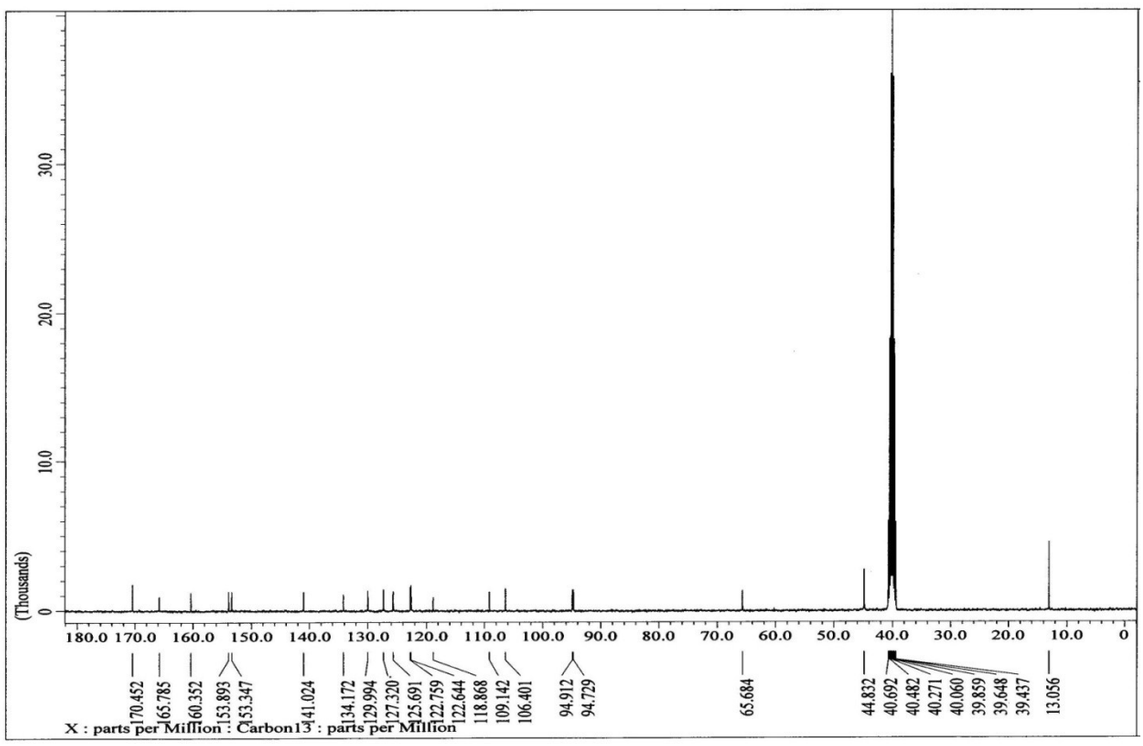

Fig. S4. ^{13}C NMR of **4**

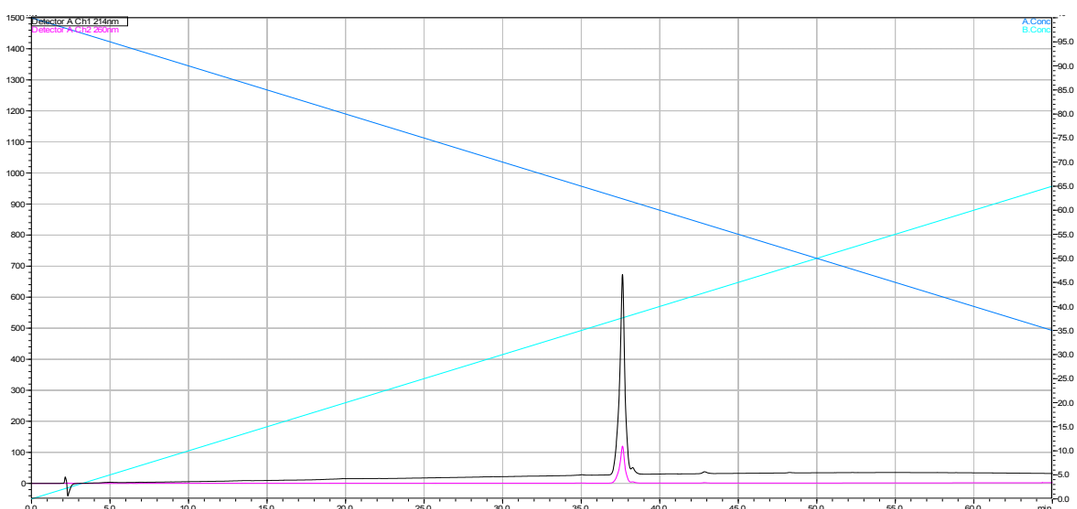

Fig. S5. HPLC chromatogram of **1**

+MS, 0.3-0.5min #19-28

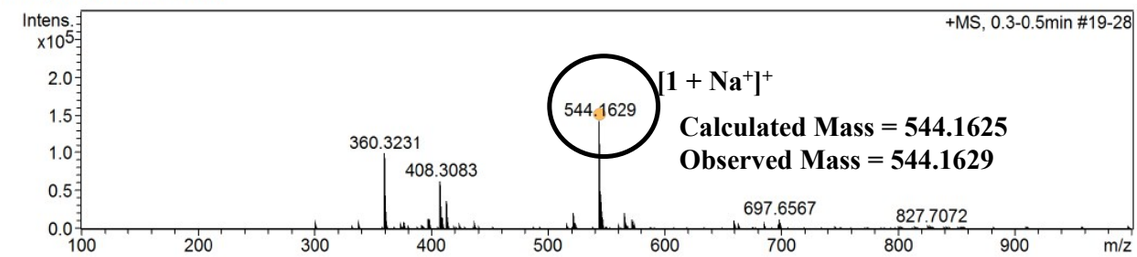

Meas. m/z	#	Ion Formula	m/z	err [ppm]	mSigma	# Sigma	Score	rdb	e¯ Conf	N-Rule
544.1629	1	C29H22N9OS	544.1663	-6.1	3.5	1	17.11	23.5	even	ok
	2	C28H26N5O5S	544.1649	3.6	7.4	2	52.83	18.5	even	ok
	3	C27H30NO9S	544.1636	1.2	17.8	3	100.00	13.5	even	ok
	4	C31H30NO4S2	544.1611	-3.4	24.4	4	40.24	17.5	even	ok
	5	C28H34NO4S3	544.1644	2.8	41.8	5	33.66	12.5	even	ok
	1	C31H27N3NaO3S	544.1665	6.6	4.1	1	14.77	19.5	even	ok
	2	C27H23N9NaOS	544.1638	-1.7	8.5	2	97.71	20.5	even	ok
	3	C26H27N5NaO5S	544.1625	0.8	19.4	3	100.00	15.5	even	ok
	4	C25H31NNaO9S	544.1612	3.3	27.6	4	47.14	10.5	even	ok
	5	C26H35NNaO4S3	544.1620	-1.7	41.1	5	57.91	9.5	even	ok

Fig. S6. HRMS (ESI-TOF) spectrum of **1**

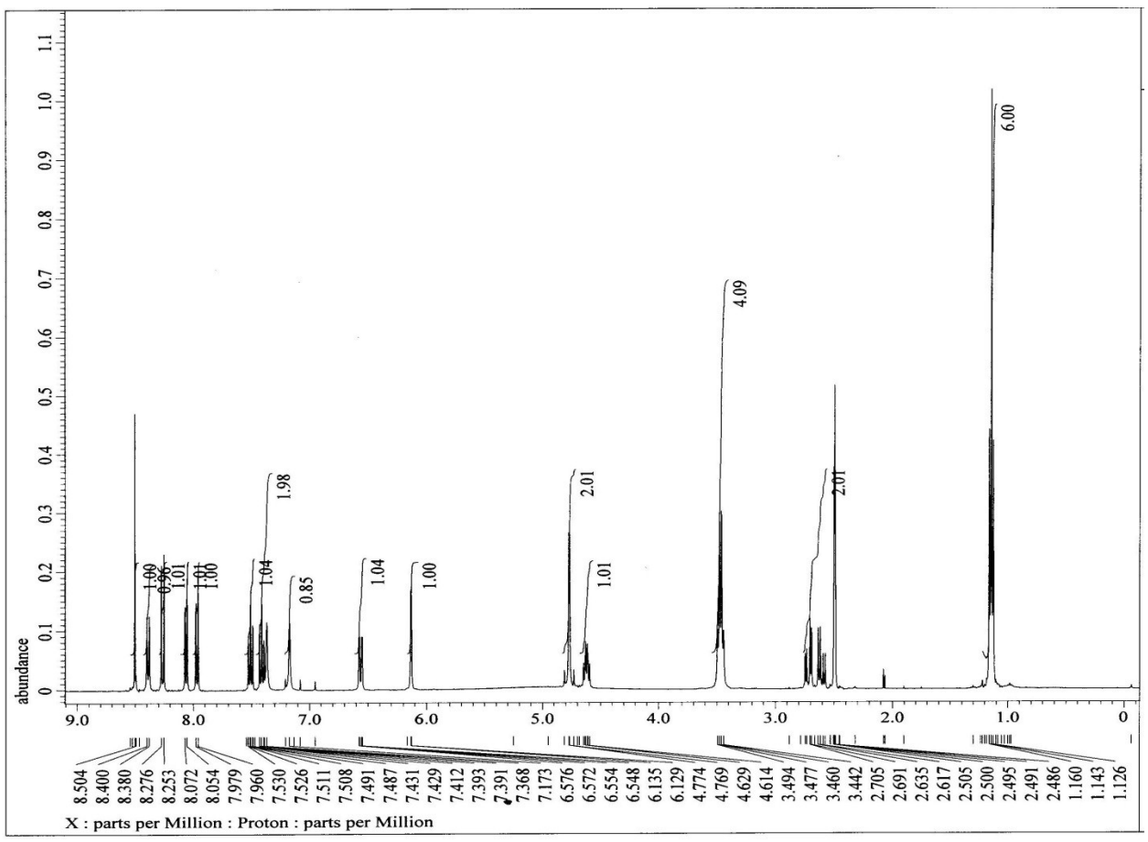
abundance
9.0
8.0
7.0
6.0
5.0
4.0
3.0
2.0
1.0
0
1.00
0.96
1.01
1.01
1.00
1.04
1.98
0.85
1.04
1.00
2.01
1.01
4.09
2.01
6.00
8.504
8.400
8.380
8.276
8.253
8.072
8.054
7.979
7.960
7.530
7.526
7.511
7.508
7.491
7.487
7.431
7.429
7.412
7.393
7.391
7.368
7.173
6.576
6.572
6.554
6.548
6.135
6.129
4.774
4.769
4.629
4.614
3.494
3.477
3.460
3.442
2.705
2.691
2.635
2.617
2.505
2.500
2.495
2.491
2.486
1.160
1.143
1.126
X : parts per Million : Proton : parts per Million

Fig. S7. ^{1}H NMR of **1**

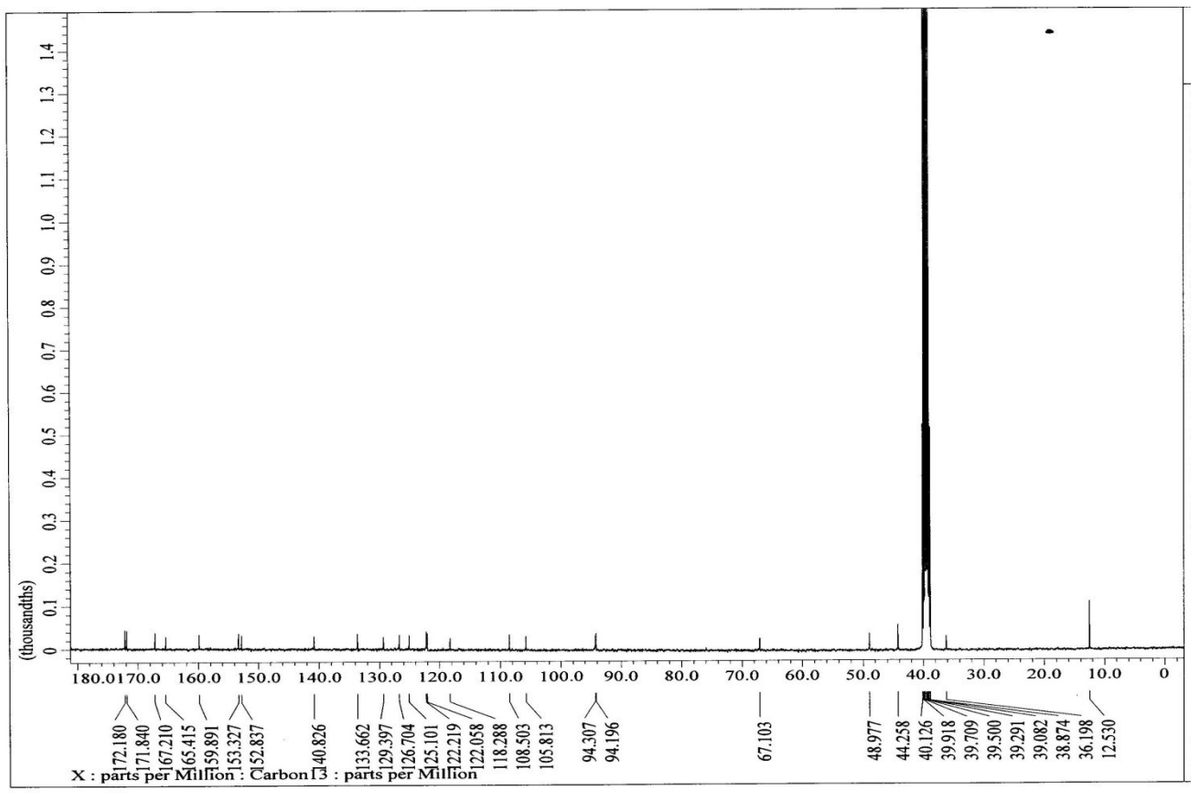

Fig. S8. ^{13}C NMR of **1**

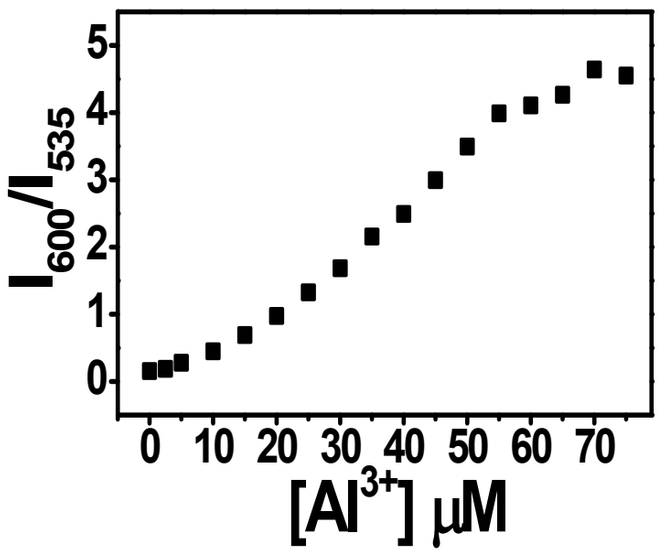

Fig. S9. Intensity ratio change (I_{600}/I_{535}) of **1** (5 μM) as a function of Al^{3+} in aqueous buffered solution (10 mM Tris, pH 7.0) (λ_{ex} = 470 nm).

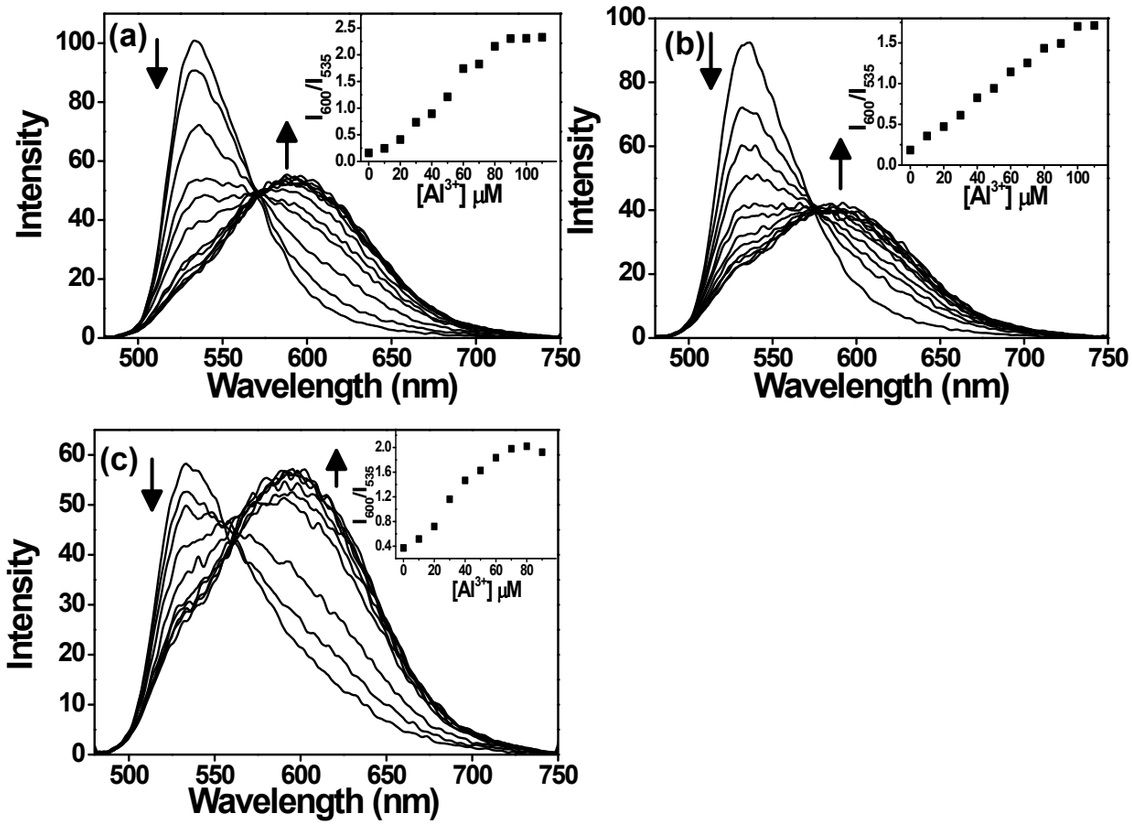

Fig. S10. Fluorescence emission spectra of **1** (5 μM) with increasing concentration of Al^{3+} in the presence of (a) Cu^{2+} (12 equiv), (b) Cr^{3+} (12 equiv) and (c) Fe^{3+} (12 equiv) in aqueous buffered solution (10 mM Tris, pH 7.0).

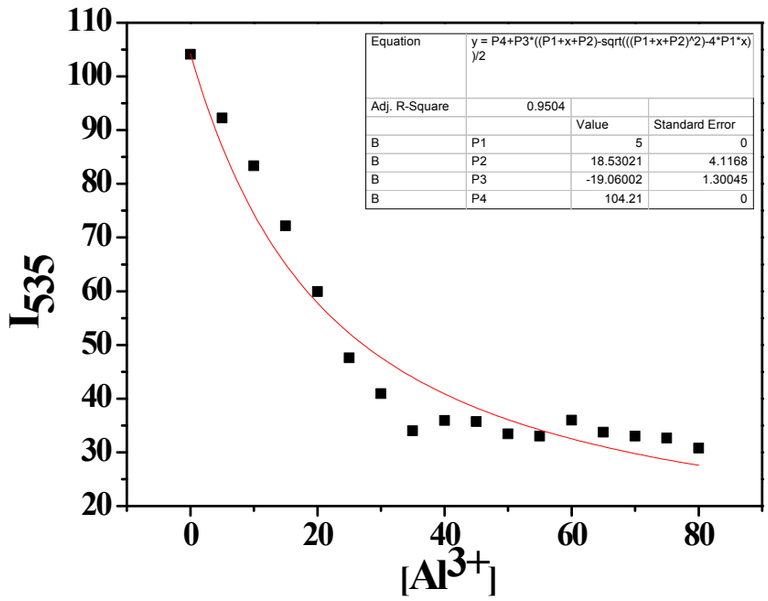

Fig. S11. Non-linear least-squares fitting of the emission intensity of **1** (5 μM) with increasing concentration of Al^{3+} in aqueous buffered solution (10 mM Tris, pH 7.0).

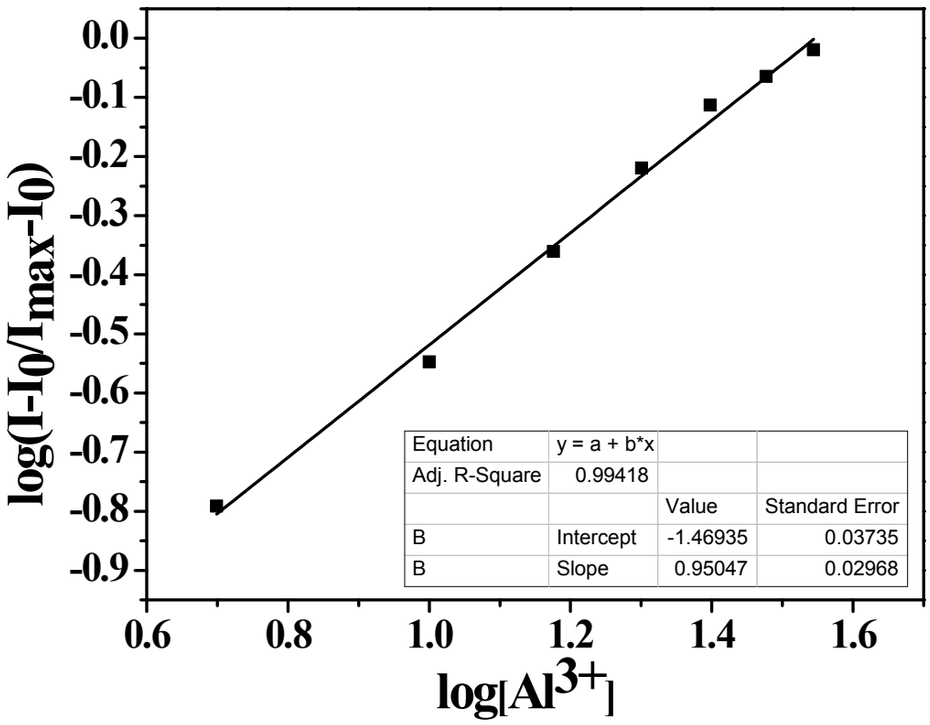

Figure S12. Benesi-Hildebrand plot for determination of the binding stoichiometry and binding constant of **1** (5 μM) for Al^{3+} in aqueous buffered solution (10 mM Tris, pH 7.0). Emission intensity at 535 nm was used in the plot.

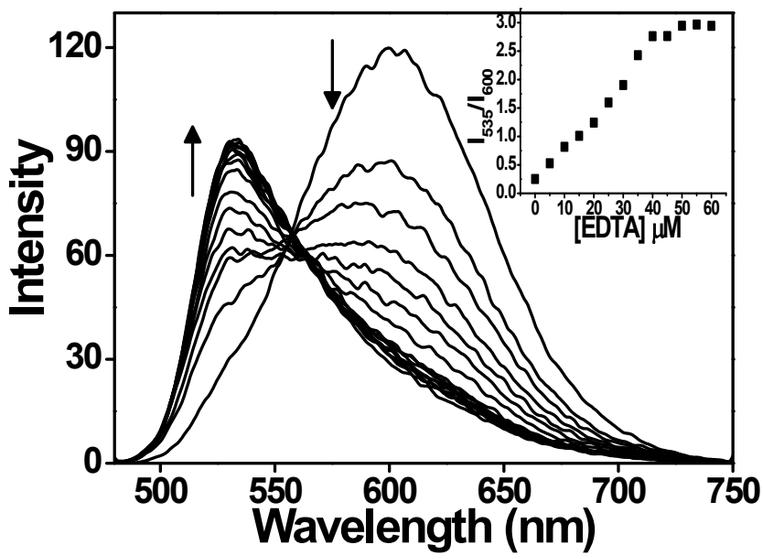

Fig. S13. Fluorescence emission spectra of **1** (5 μM) with Al^{3+} (12 equiv) in the presence of increasing concentration of EDTA in aqueous buffered solution (10 mM Tris, pH 7.0) (λ_{ex} = 470 nm, slit = 12/10 nm).

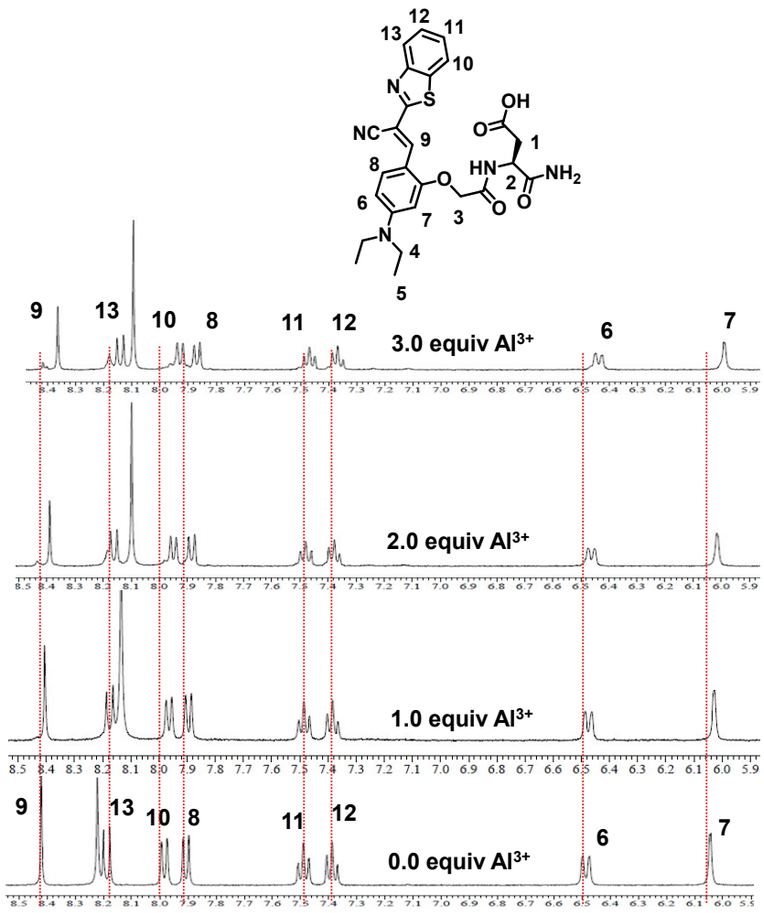

Fig. S14. Partial ^{1}H NMR spectra (400 MHz) of **1** (5 mM) with increasing concentration of Al^{3+} in DMSO-d_6/D_2O (v/v = 4:1) containing 10 mM ammonium formate.

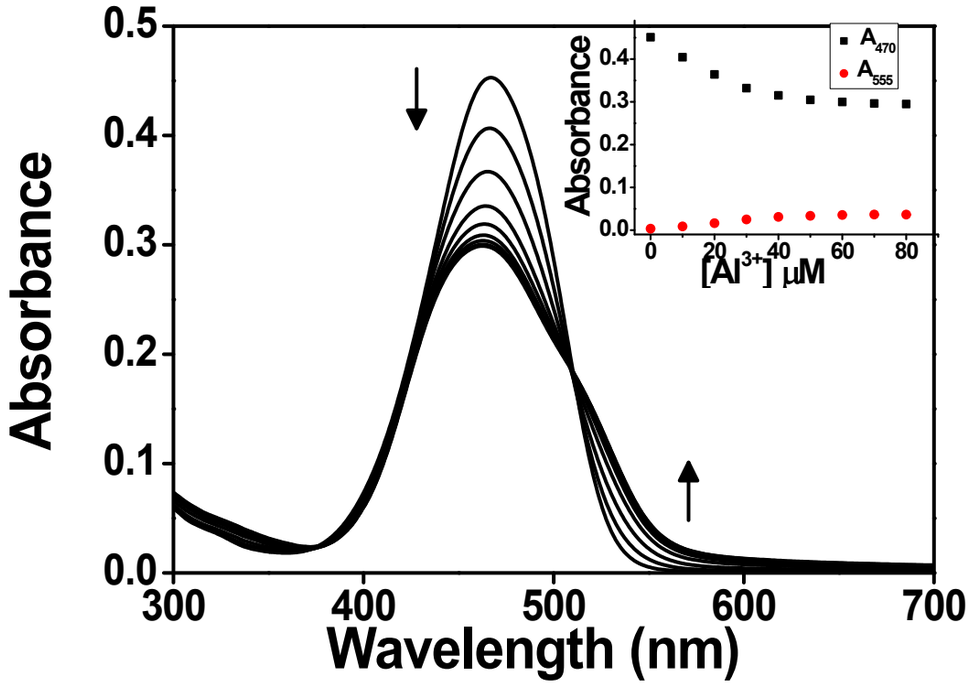

Fig. S15. UV-vis absorption spectra of **1** (5 μM) upon the gradual addition of Al^{3+} (0-80 μM) in aqueous buffered solution (10 mM Tris, pH 7.0).

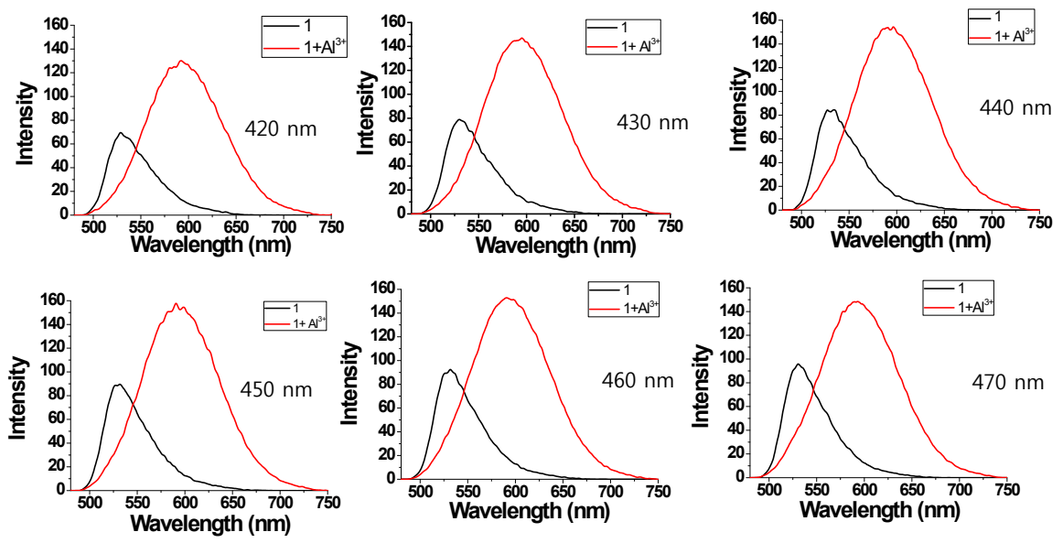

Fig. S16. Fluorescence spectra of **1** (5 μM) in the absence and presence of Al^{3+} (12 equiv) with a different excitation wavelength

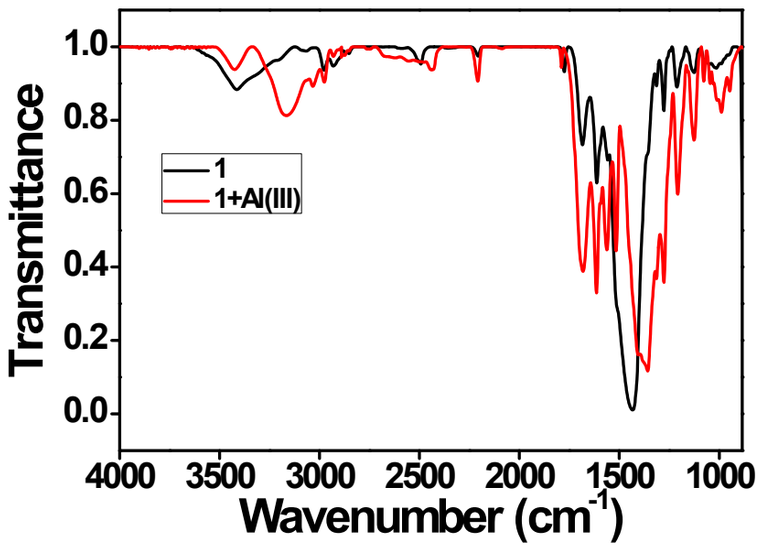

Fig. S17. IR spectra of **1** in the absence and presence of Al^{3+}.

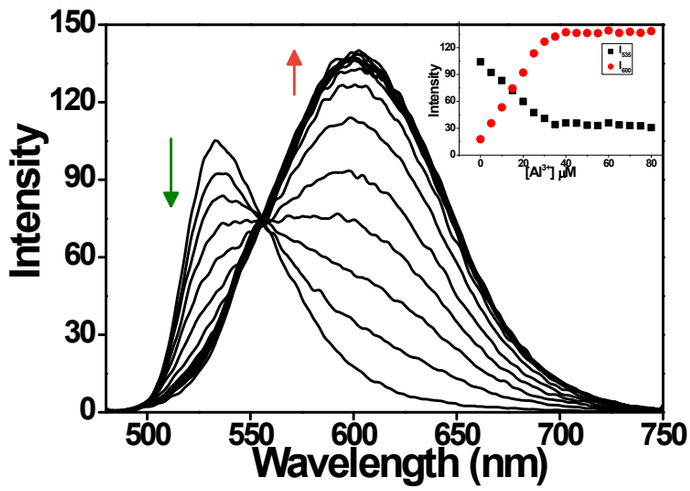

Fig. S18. Fluorescence spectra of **1** (5 μM) with increasing concentration of Al^{3+} in aqueous buffered solution (10 mM Hexamine buffer, pH 6.0).

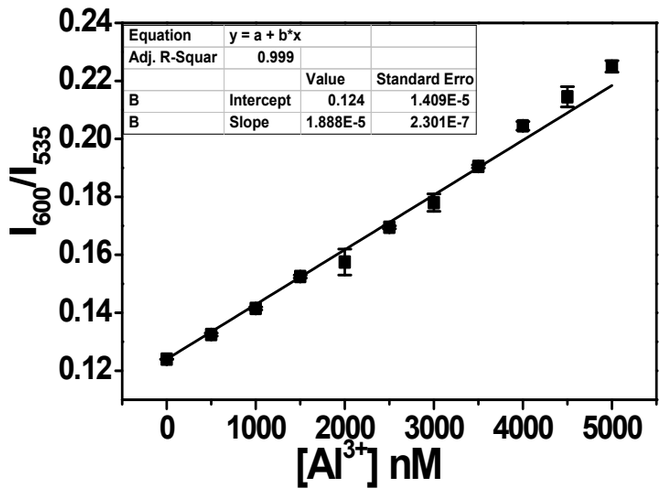

Fig. S19. Linear relationship between the emission intensity ratio (I_{600}/I_{535}) of **1** (5 μM) and the concentration of Al^{3+} (0-5000 nM) in aqueous buffered solution (10 mM Tris, pH 7.0).

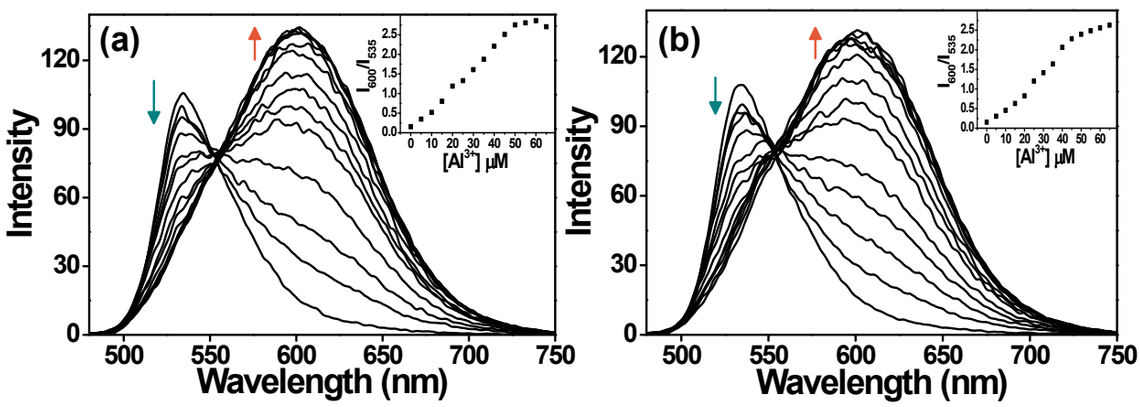

Fig. S20. Fluorescence emission spectra of **1** (5 μM) with increasing concentration of Al^{3+} (0−65 μM) in aqueous buffered solution (10 mM Tris, pH 7.0) containing (a) 10 % (v/v) tap water and (b) 10 % (v/v) ground water (λ_{ex} = 470 nm).

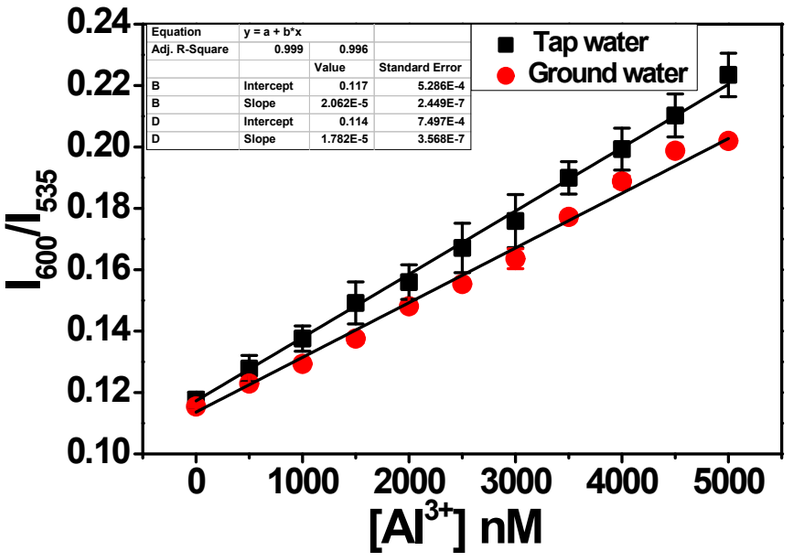

Fig. S21. Linear relationship between the emission intensity ratio (I_{600}/I_{535}) of **1** (5 μM) and the concentration of Al^{3+} (0-5000 nM) in aqueous buffered solution (10 mM Tris, pH 7.0) containing 10 % (v/v) tap water and 10% (v/v) groundwater, respectively.

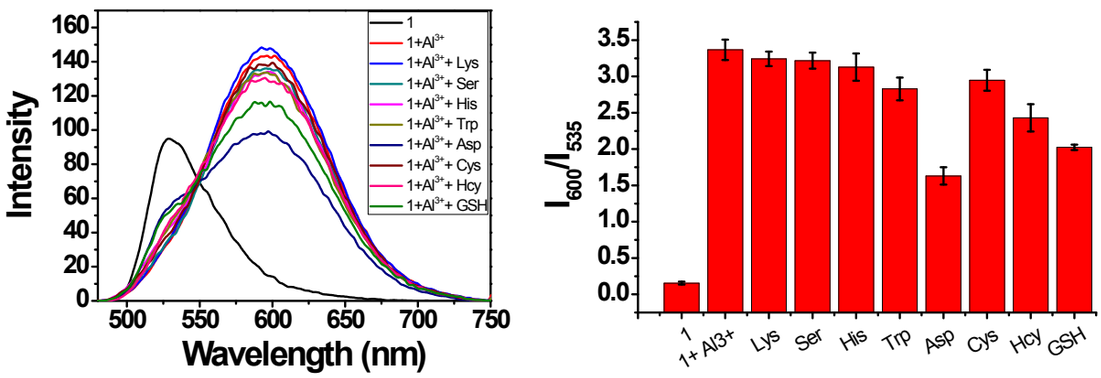

Fig. S22. Fluorescence emission spectra of **1** (5 μM) with Al^{3+} (12 equiv) in the presence of amino acids (100 μM) and biothiols (100 μM).

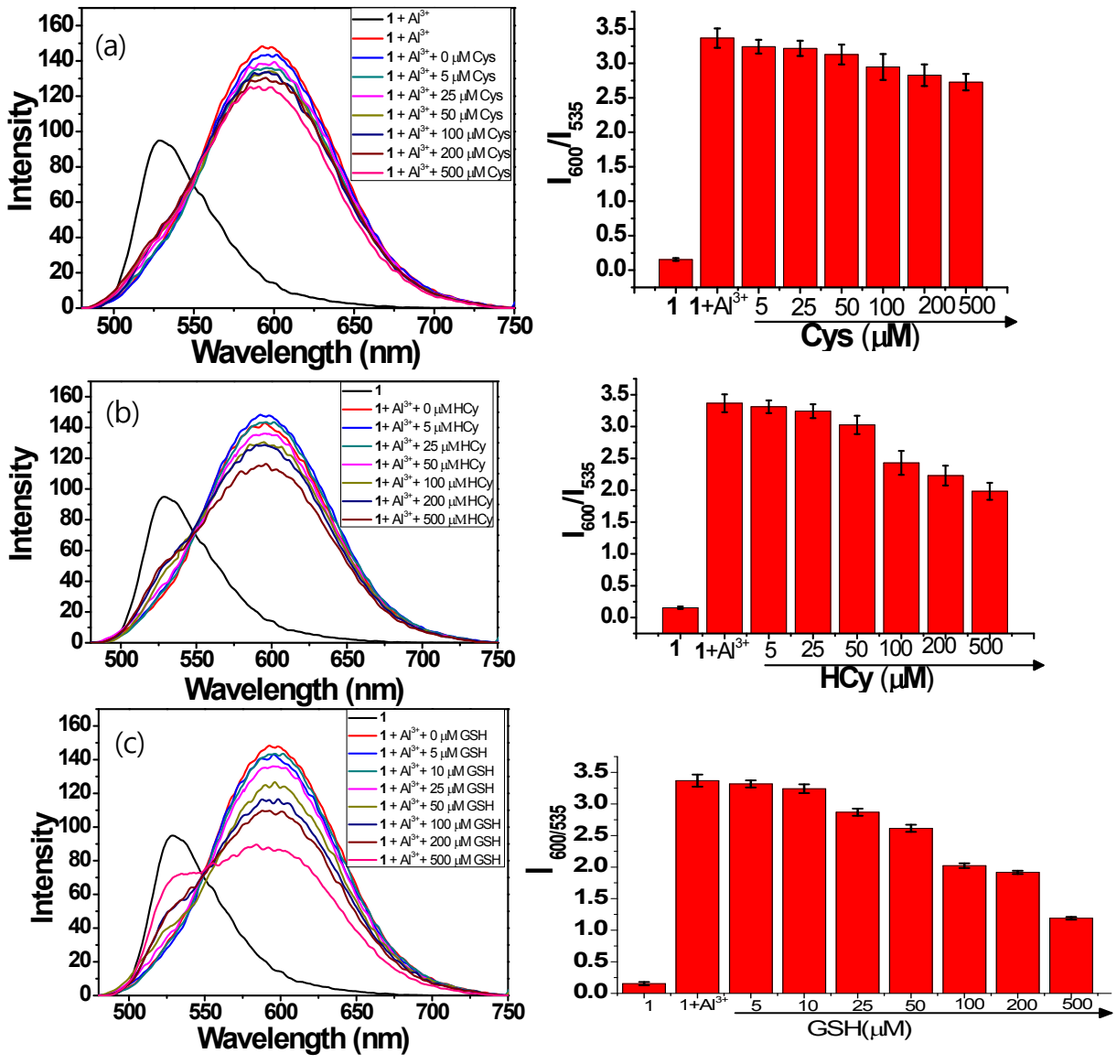

Fig. S23. Fluorescence emission spectra of **1** (5 μM) in the presence of Al^{3+} (12 equiv) with increasing concentration of (a) Cys, (b) Hcy, and (c) GSH.

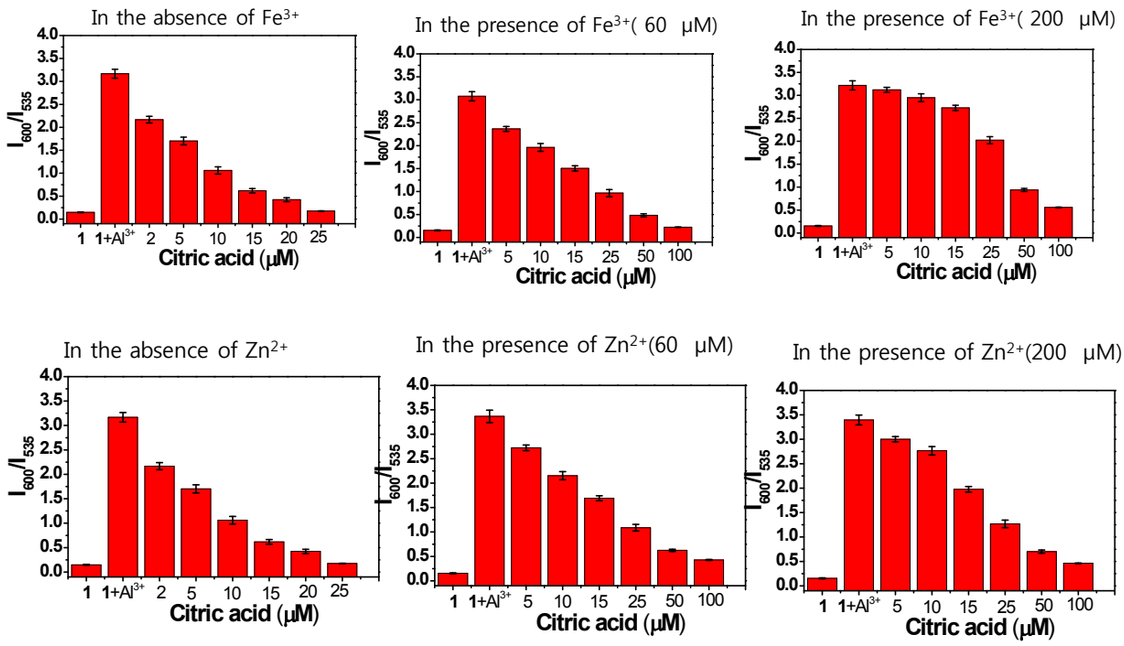

Fig. S24. Emission intensity ratio changes of **1** (5 μM) by Al^{3+} (12 equiv) in the presence of (a) citric acid with Fe^{3+} and (b) citric acid with Zn^{2+}.

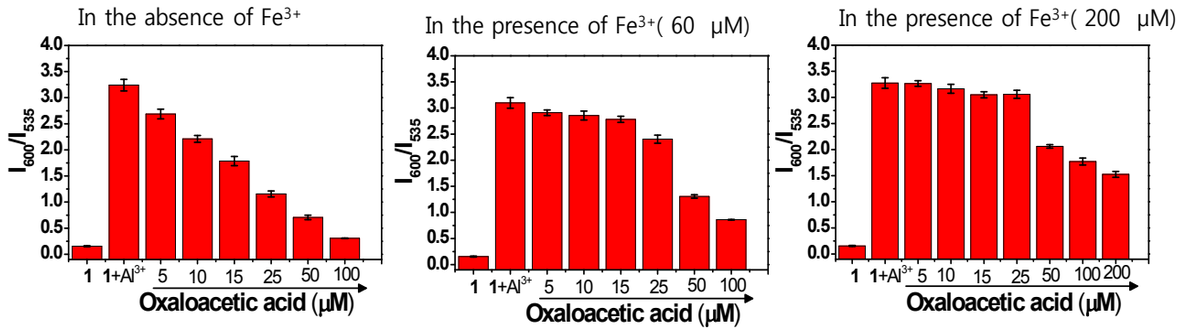

Fig. S25. Emission intensity ratio changes of **1** (5 μM) by Al^{3+} (12 equiv) in the presence of ~~oxalic acid~~ and Fe^{3+}.

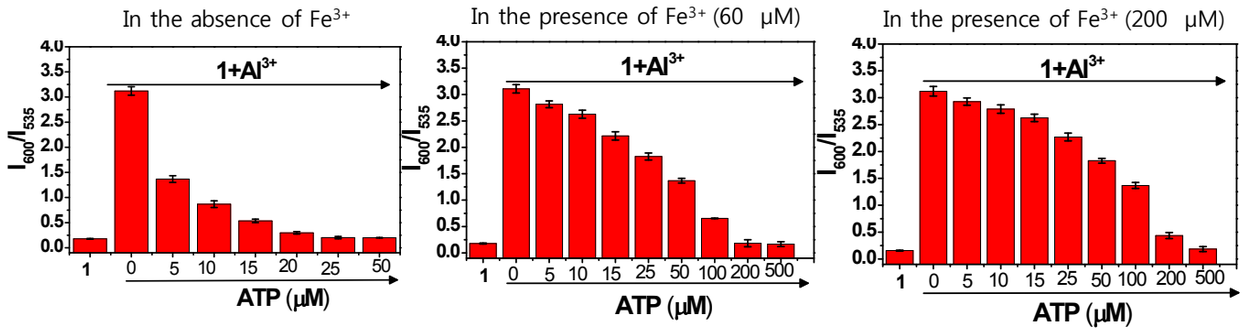

Fig. S26. Emission intensity ratio changes of **1** (5 μM) by Al^{3+} (12 equiv) in the presence of ATP and Fe^{3+} .

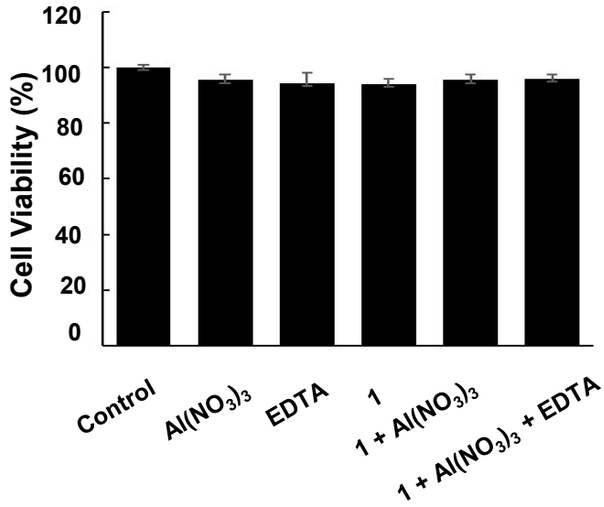

Fig. S27. MTT assay for the viability of MDA-MB-231 cells in DMEM 10% FBS treated with **1**, **1** + $Al(NO_3)_3$ and **1** + $Al(NO_3)_3$ + EDTA for 24 h. The results are based on three separate MTT assays. The concentration of **1**, $Al(NO_3)_3$ and EDTA is 10 μM, 50 μM and 200 μM, respectively.

References

1 G. L. Long and J. D. Winefordner, *Anal. Chem*., 1983, **55**, 712A−724A.

2 R. Reddi, T. R. Guzman, R. M. Breece, D. L. Tierney and B. R. Gibney, *J. Am. Chem. Soc*., 2007, **129**, 12815–12827.

3 H. Y. Lin, P. Y. Cheng, C. F. Wan and A. T. Wu, *Analyst*, 2012, **137**, 4415−4417.

4 A. Roy, S. Dey and P. Roy, *Sens. Actuators B*, 2016, **237**, 628−642.

5 L. Porres, A. Holland, L.-O. Palsson, A. P. Monkman, C. Kemp and A. Beeby, *J. Fluores*., 2006, **16**, 267−272.

6 G. A. Vehar, A. V. Reddy and J. H. Freisheim, *Biochemistry*, 1976, **15**, 2512−2518.